POWDERS OF CHROMIUM AND CHROMIUM CARBIDES OF DIFFERENT MORPHOLOGY AND NARROW SIZE DISTRIBUTION

S. Loubière, Ch. Laurent,* J.P. Bonino, and A. Rousset
Laboratoire de Chimie des Matériaux Inorganiques, ESA CNRS 5070,
Université Paul-Sabatier, 31062 Toulouse Cedex 4, France

ABSTRACT

Powders of Cr and Cr carbides (Cr_2C, Cr_7C_3, and $Cr_{23}C_6$) have been prepared by hydrogen reduction of $CrO_{1.9}$ and Cr_3C_2 powders of different morphology, texture and specific surface area. The Cr and Cr carbides particles have the morphology of the parent compound and a narrow size distribution. Depending on the shape, the average size is of the order of some micrometers or some tens of micrometers. Starting with Cr_3C_2 allows the preparation of Cr powders at a temperature (1000°C) markedly lower than that required when $CrO_{1.9}$ is used as the precursor (1300°C). However, a Cr_3C_2 specific surface area of the order of 10 m^2/g is necessary to achieve this within a reasonably short time (6 to 12 h). Powders of the lower carbides are prepared by using a milder hydrogen thermal treatment.

KEYWORDS: A. carbides, A. oxides

INTRODUCTION

Micrometric metal and carbide powders of controlled morphology and uniform size distribution are of considerable interest for industrial applications such as conductive inks or pastes for electronic materials and also for powder metallurgy [1–4]. Metals such as Fe, Co, Ni, Cu, and Ru and the noble metals have been prepared by reduction of the appropriate precursor compounds, using notably the so-called polyol process [5], the precipitation from homogeneous solutions [6], and the microwave-hydrothermal method [7]. An alternative to

*To whom correspondence should be addressed.

these wet routes is the reduction in H_2 or CO atmosphere of solid precursors which already are monodispersed and of a definite shape. As pointed out by Matijevic [6], such conversions can take place without a loss in the morphology or the dispersion of the final products only under carefully controlled conditions. Thus, in contrast to the above-mentioned metals, a Cr powder is very difficult to obtain by such methods, because of the difficulty in reducing Cr_2O_3. Thibaudon et al. [8] have shown that decarburization in hydrogen of Cr_3C_2 yields the lower carbides Cr_7C_3 and $Cr_{23}C_6$ and even Cr if the treatment is severe enough (1000°C, 150 h); however, they did not investigate powder characteristics such as morphology and particle size.

Lerch and Rousset [9] have shown that the pseudomorphic decomposition in air of chromium oxalates of controlled morphology (needles, rods, polyhedra, and spheres) could lead to metastable chromium oxides of general formula $CrO_{1.9}$ with the same morphology. These products have a specific surface area in the 200–350 m^2/g range and it has been shown in previous works [10,11] that they are interesting precursors for the synthesis of the stable Cr_3C_2 and metastable Cr_3C_{2-x} phases of controlled morphology while combining the advantages of moderate preparation temperature (700°C) and high yield. The aim of the present paper is to investigate the synthesis of Cr_2C, Cr_7C_3, $Cr_{23}C_6$, and Cr powders of different morphology and narrow size distribution using $CrO_{1.9}$ and Cr_3C_2 as starting materials.

EXPERIMENTAL

The synthesis of the oxalates and $CrO_{1.9}$ oxides was described in detail in previous papers [9,10]. Briefly, ammonium trioxalatochromate(III) $(NH_4)_3[Cr(C_2O_4)_3]$ was prepared by mixing the appropriate amounts of ammonium oxalate $(NH_4)_2(C_2O_4)\cdot 2H_2O$ and chromium(III) nitrate $Cr(NO_3)_3\cdot 9H_2O$ in an aqueous solution heated at 60°C. The clear solution obtained was cooled to room temperature and rapidly added to an organic solution (equivolumic mixture of either acetone and methanol or ethanol and ethyleneglycol), in which precipitation occurred immediately. Oxalates of different morphology, namely, needles, rods, polyhedra, and spheres (more precisely, spherical agglomerates of platelets), were obtained depending

TABLE 1
Morphological and Microstructural Characteristics of the Starting Oxide and Carbide Powders

Nature	Shape	S_w (m^2/g)	Average size[a] (μm)
$CrO_{1.9}$	polyhedra	185	30
$CrO_{1.9}$	spheres	320	9
Cr_3C_2	needles	10.0	70 × 10
Cr_3C_2	rods	10.0	70 × 20
Cr_3C_2	polyhedra	9.1	20
Cr_3C_2	spheres	12.0	8
Cr_3C_2	spheres	4.0	8
Cr_3C_2	spheres	1.0	8

S_w: specific surface area.
[a]Determined from measurements of SEM images.

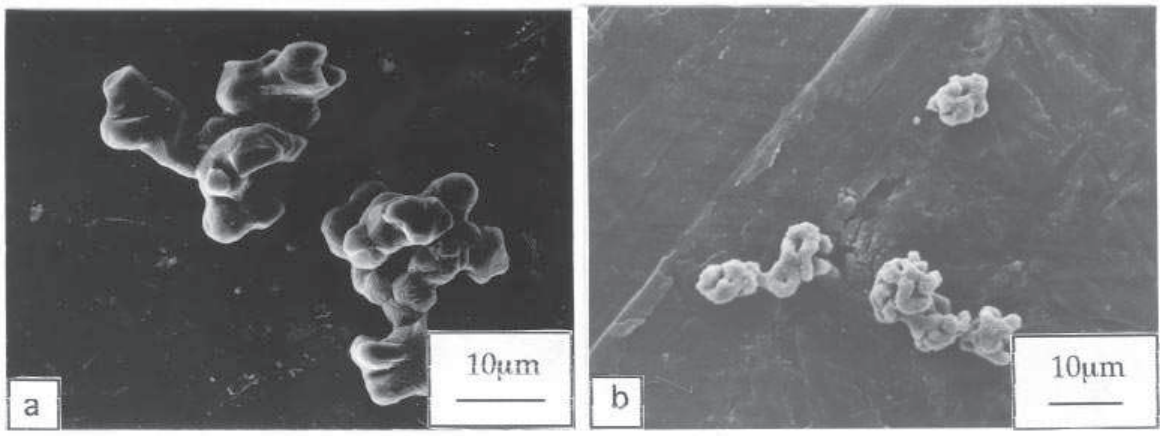

FIG. 1
SEM images showing Cr particles obtained from the polyhedral (a) and spherical (b) $CrO_{1.9}$ oxides after a H_2 reduction at 1300°C for 6 h.

on the relative proportions of aqueous and organic solutions and on the nature of the latter. After filtering and ethanol washing, the powders were oven dried at 90°C for 48 h.

Powders of the metastable chromium oxide $CrO_{1.9}$ were prepared by decomposition in air at 300°C of the chromium oxalates of different morphology [9,10]. The so-obtained oxides, which have the same morphology as the parent oxalates, were heat-treated for 2 h at 700°C in an H_2-CH_4 atmosphere (10 mol% CH_4) to yield Cr_3C_2 powders with the same morphology and a specific surface area of the order of 10 m^2/g as described elsewhere [10]. The gas flow was dried on P_2O_5 and its composition was monitored using mass flow controllers. Other specimens of the spherical Cr_3C_2 were prepared by treatments at 800 and 1000°C to obtain powders with a lower specific surface area (4 and 1 m^2/g, respectively).

The Cr_3C_2 powders as well as the polyhedral and spherical $CrO_{1.9}$ specimens were then submitted to a treatment in pure, dry H_2 at different temperatures and for different times as required for the study. The morphological and microstructural features of all the starting powders are reported in Table 1.

TABLE 2
Phases Detected by XRD After Treating the Spherical Cr_3C_2 Powders in H_2 for 2 h at Different Temperatures

Temperature (°C)	S1	S4	S12
500	Cr_3C_2	Cr_3C_2	Cr_3C_2
600	Cr_3C_2	Cr_3C_2	$Cr_3C_2 + Cr_2C$
650	Cr_3C_2	Cr_3C_2	Cr_2C
700	Cr_3C_2	Cr_3C_2	$Cr_2C + Cr_7C_3$
800	Cr_3C_2	$Cr_3C_2 + Cr_7C_3$	$Cr_2C + Cr_7C_3$
850	Cr_3C_2	$Cr_3C_2 + Cr_7C_3$	Cr_7C_3
900	$Cr_3C_2 + Cr_7C_3$	$Cr_3C_2 + Cr_7C_3$	$Cr_7C_3 + Cr_{23}C_6$
950	$Cr_3C_2 + Cr_7C_3$	Cr_7C_3	$Cr_7C_3 + Cr_{23}C_6$
1000	$Cr_3C_2 + Cr_7C_3$	Cr_7C_3	$Cr_{23}C_6$

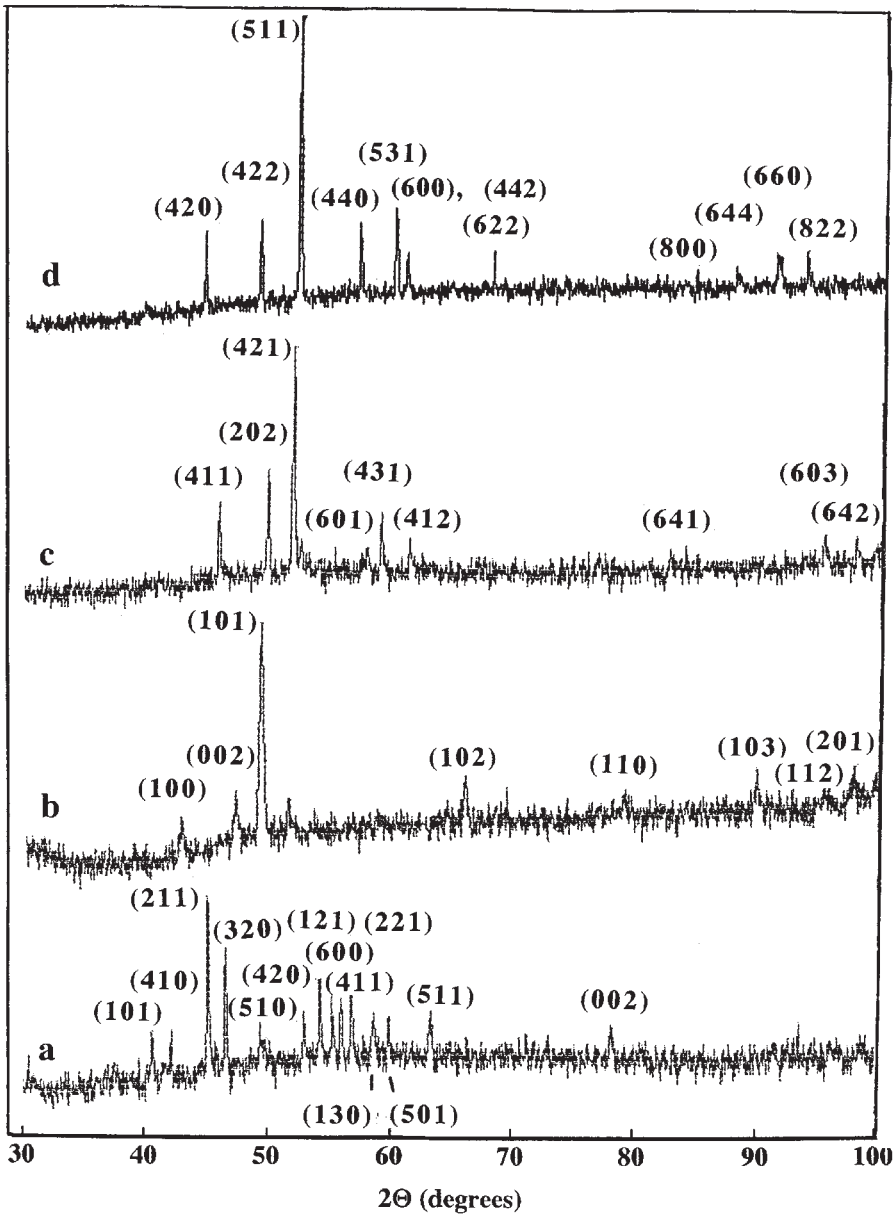

FIG. 2

XRD patterns of the products obtained from the Cr_3C_2 powder S12 heat-treated in H_2 for 2 h at (a) 500°C (Cr_3C_2), (b) 650°C (Cr_2C), (c) 850°C (Cr_7C_3), and (d) 1000°C ($Cr_{23}C_6$).

The resulting materials were studied by scanning electron microscopy (SEM) and X-ray diffraction (XRD) using Co Kα radiation (λ = 0.17902 nm). The specific surface areas were measured by the BET method using N_2 adsorption at liquid N_2 temperature. Chemical analyses were performed by atomic absorption.

RESULTS AND DISCUSSION

Starting from the $CrO_{1.9}$ oxides, it was only possible to obtain Cr particles containing less than 0.5 wt% of oxygen with a H_2 reduction after 6 h at a temperature as high as 1300°C.

TABLE 3
Phases Detected by XRD after Treating the Cr_3C_2 Powders in H_2 at 1000°C for Different Times

Dwell time (h)	Spheres	Needles and rods	Polyhedra
1	$Cr_{23}C_6$	Cr_7C_3	Cr_7C_3
2	$Cr_{23}C_6$	$Cr_7C_3 + Cr_{23}C_6$	$Cr_7C_3 + Cr_{23}C_6$
4	$Cr_{23}C_6 + Cr$	$Cr_7C_3 + Cr_{23}C_6$	$Cr_7C_3 + Cr_{23}C_6$
5	$Cr_{23}C_6 + Cr$	$Cr_{23}C_6$	$Cr_7C_3 + Cr_{23}C_6$
6	Cr	$Cr_{23}C_6 + Cr$	$Cr_{23}C_6$
8	—	$Cr_{23}C_6 + Cr$	$Cr_{23}C_6 + Cr$
10	—	Cr	$Cr_{23}C_6 + Cr$
12	—	—	Cr

Furthermore, SEM observations (Fig. 1) show that the so-obtained Cr particles exhibit an ill-defined morphology, which is due to some sintering during the treatment. No difference in the reduction behavior was observed between the polyhedral and spherical powders despite the difference in specific surface area (185 and 320 m^2/g, respectively).

The spherical Cr_3C_2 powders of different specific surface area (1, 4, and 12 m^2/g, hereafter denoted as powders S1, S4, and S12, respectively) were heat-treated in H_2 for 2 h at different temperatures ranging between 500 and 1000°C. The phases detected by XRD patterns analysis are reported in Table 2. When starting from the S1 Cr_3C_2 powder, Cr_3C_2 is still the only phase detected in the XRD patterns of products reduced a temperatures lower than 900°C. A mixture of Cr_3C_2 and Cr_7C_3 is detected for specimens reduced at 900, 950, and 1000°C. Starting from S4, Cr_7C_3 is detected in addition to Cr_3C_2 after the 800, 850, and 900°C treatments and is the sole phase detected after the 950 and 1000°C treatments. As expected, the reactivity of the S12 powder is higher than that of S1 or S4. Indeed, the S12 Cr_3C_2 (Fig. 2a) is gradually transformed into Cr_2C, which is the sole product detected in the powder treated at 650°C (Fig. 2b). Cr_2C is then transformed into Cr_7C_3 (obtained at 850°C, Fig. 2c), which in turn yields $Cr_{23}C_6$ at 1000°C (Fig. 2d).

In agreement with Leclercq et al. [12], we observed that decarburization occurs before a complete removal of the excess free carbon; indeed, the amount of free carbon in the S12 Cr_3C_2 was found to be 1.5 wt%, whereas it decreases to 0.8 wt% in the product treated at 500°C, 0.3 wt% in Cr_2C, and 0 wt% in Cr_7C_3 and $Cr_{23}C_6$. It should be noted that the proportion of extra carbon in our Cr_3C_2 powder is much lower than that reported by Leclercq et al. [12].

To achieve the obtention of Cr at 1000°C, the S12 spherical Cr_3C_2 and the differently shaped Cr_3C_2 powders (needles, rods and polyhedra), which have a similar specific surface area (ca. 10 m^2/g), were heat-treated in H_2 for different times ranging between 1 and 12 h. The results are summarized in Table 3 and the XRD patterns of the powders obtained from the spherical carbide are shown in Figure 3.

Whatever the morphology of the starting Cr_3C_2 powder, it is possible to prepare Cr_7C_3, $Cr_{23}C_6$, and Cr, or to obtain mixtures of these compounds, depending on the dwell time. It appears that the spheres and polyhedra are the most and least reactive powders, respectively, and that the needles and rods have an intermediate behavior upon reduction, similar to each other. Indeed, $Cr_{23}C_6$ is obtained after treatments of 1 h (spheres), 5 h (needles and rods), and

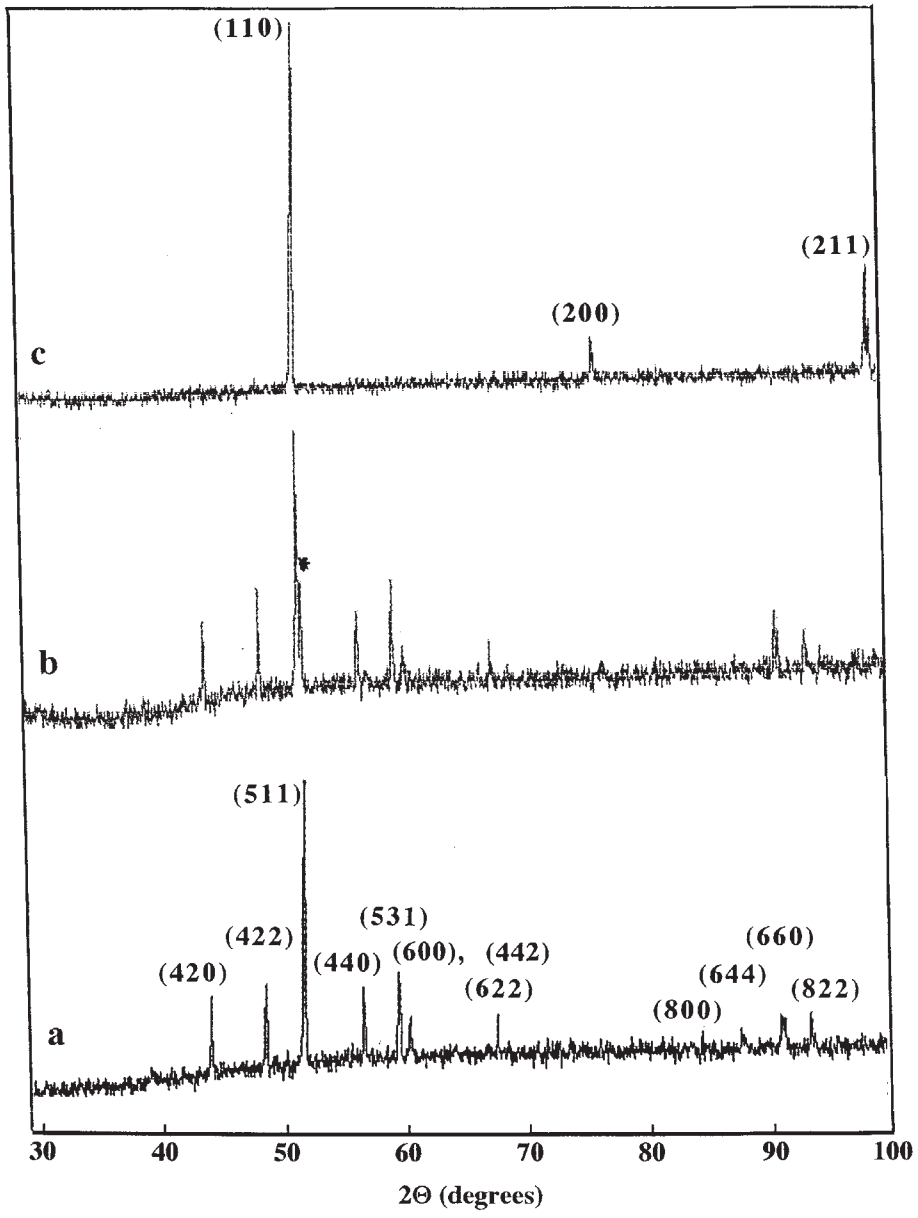

FIG. 3

XRD patterns of some of the products obtained from the spherical Cr_3C_2 powder S12 heat-treated in H_2 at 1000°C for (a) 1 h ($Cr_{23}C_6$), (b) 4 h ($Cr_{23}C_6$ + Cr), and (c) 6 h (Cr).

6 h (polyhedra), and Cr is obtained after treatments of 6 h (spheres), 10 h (needles and rods), and 12 h (polyhedra).

The pseudomorphic nature of the transformation is evidenced by SEM observations. Indeed, we obtained Cr_7C_3, $Cr_{23}C_6$, and Cr powders in the shape of needles, rods, polyhedra, and spheres (Fig. 4). The Cr needles and rods are, however, very similar to each other. The size distribution seems rather narrow and the powders are not aggregated. The particle size distributions (in number) were derived from measurements of SEM images (Fig. 5). Depending on the shape, the average particle size is of the order of some micrometers (polyhedra, spheres) or some tens of micrometers (needles, rods). The length distribution of the Cr_3C_2 and Cr powders in the form of needles and rods (Figs. 5a, b, e, and f) is, in fact,

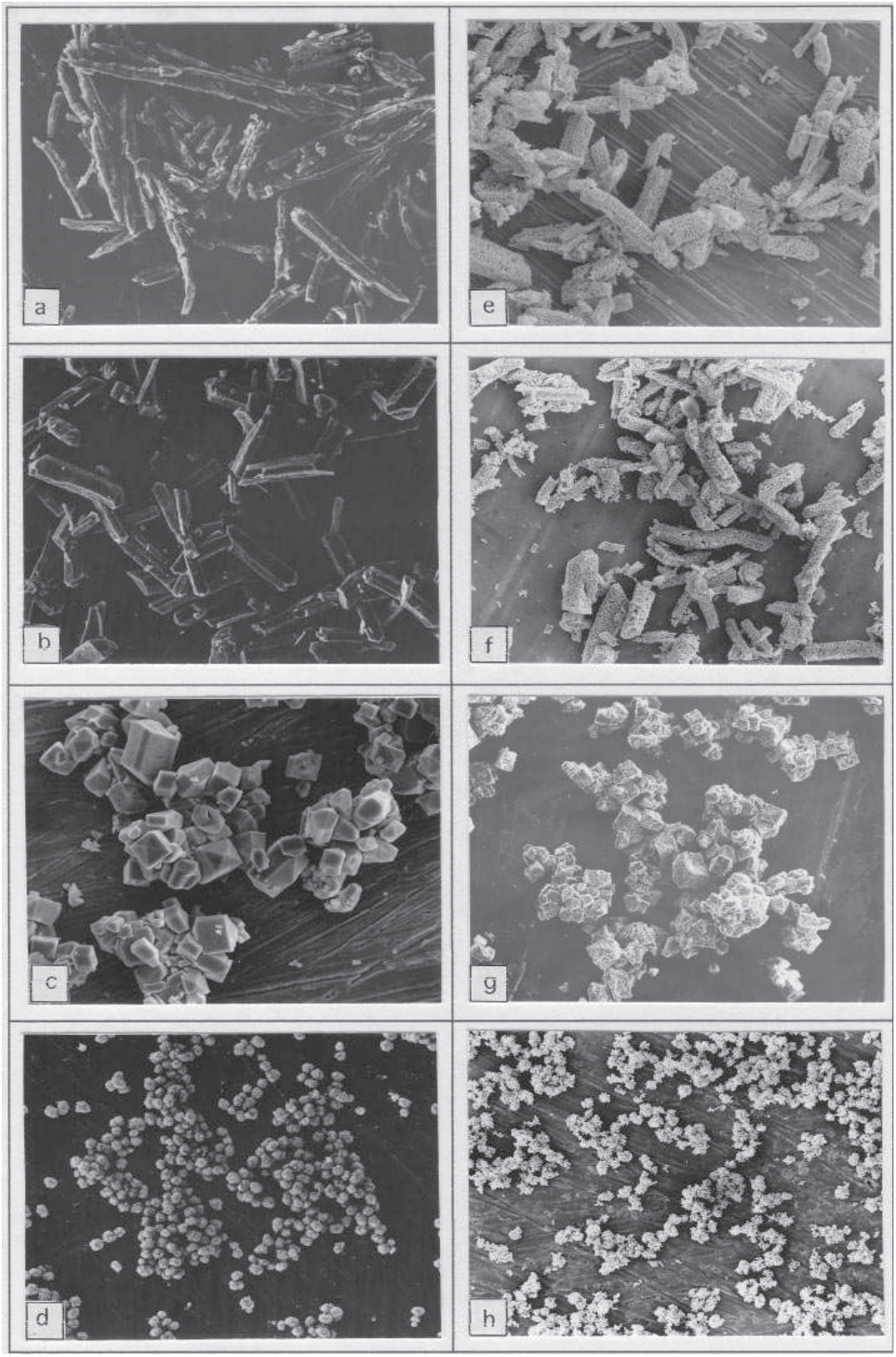

FIG. 4

SEM images of Cr_3C_2 powders showing different shapes—needles (a), rods (b), polyhedra (c), and spheres (d)—and the corresponding Cr powders (e, f, g, and h, respectively). The Cr needles and rods are very similar.

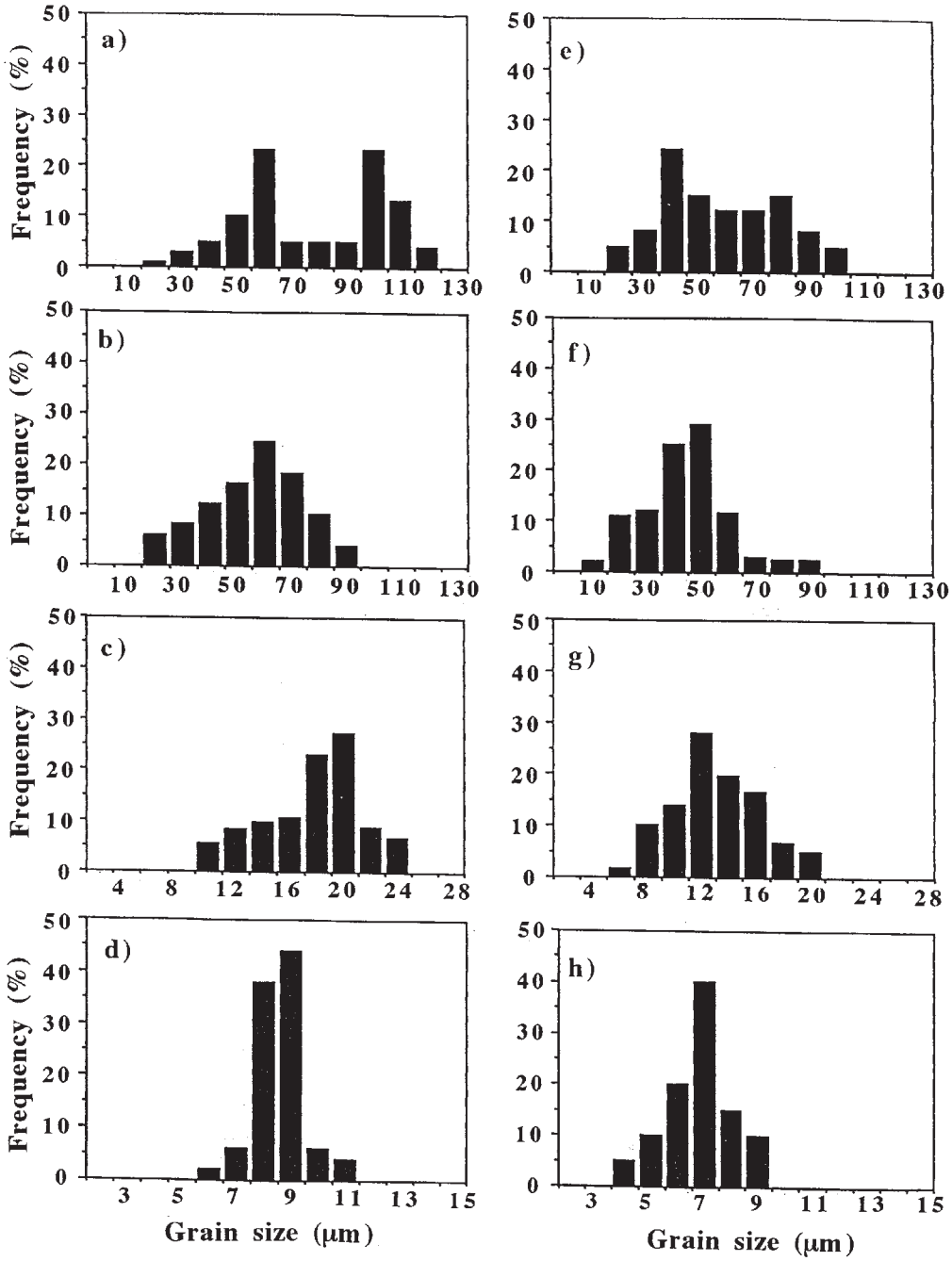

FIG. 5

Size distribution of the different Cr_3C_2 powders—needles (a), rods (b), polyhedra (c), and spheres (d)—and the corresponding Cr powders (e, f, g, and h, respectively).

large and bimodal because some needles/rods have been broken at some point during the manipulations. The size distribution is much narrower for the polyhedra and, in particular, for the spheres (Figs. 5c, d, g, h).

The Cr particles are slightly smaller than those of the parent Cr_3C_2, because the reduction treatment provokes a coalescence of the primary crystallites, in addition to the decarburization, on the one hand, and a shrinkage of the grains, on the other hand, as shown in the case

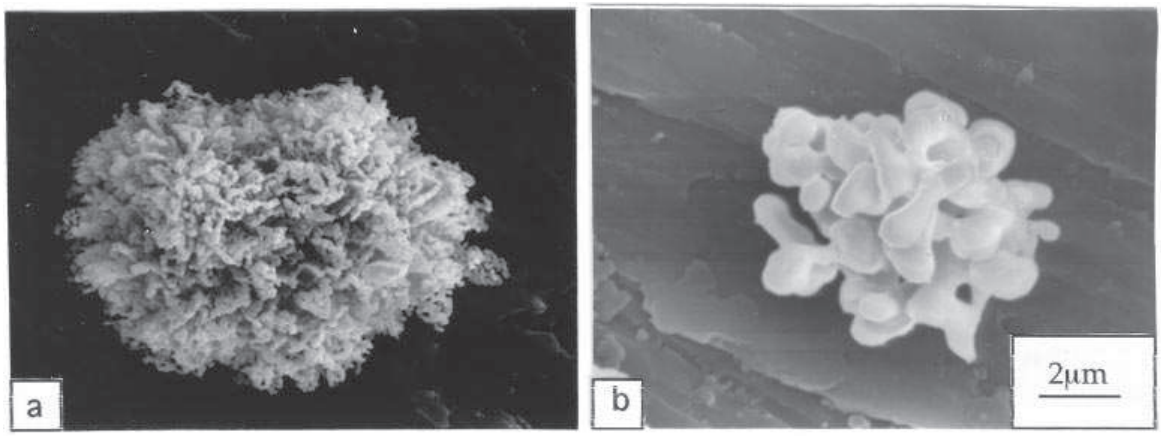

FIG. 6
Higher magnification SEM images showing the spherical Cr_3C_2 (a) and Cr powders (b).

of spheres by SEM observations (Fig. 6). It should be noted that the average size of a given powder ($CrO_{1.9}$, Cr_3C_2, Cr_2C, Cr_7C_3, $Cr_{23}C_6$, or Cr) depends on that of the parent Cr oxalate, which can be varied by minor modifications of the precipitation process.

The difference in reactivities among the various Cr_3C_2 powders is not due to differences in their specific surface areas, which are similar to each other (ca. 10 m^2/g, Table 1), but rather in their texture. Indeed, in contrast to the other specimens, which are more monolithical, the spherical grains are made up of fine crystallites (100 nm) forming a kind of "gypsum flower" texture (Fig. 6a), favor H_2 diffusion and removal of the gaseous species in this material. Similar results were observed for the reoxidation behavior of the Cr_3C_2 powders [10].

CONCLUSIONS

Powders of different morphology (needles, rods, polyhedra and spheres) of the metastable chromium oxide $CrO_{1.9}$ and of Cr_3C_2 have been prepared by the appropriate heat treatments of the corresponding Cr oxalate precursors. The hydrogen treatment of Cr_3C_2 allows preparation of Cr powders at a temperature (1000°C) markedly lower than that required when $CrO_{1.9}$ is used as the starting material (1300°C). A carbide specific surface area of the order of 10 m^2/g is necessary to achieve this within a reasonably short time (6–12 h). Due to these relatively mild experimental conditions, it is possible to obtain Cr powders of tailored morphology and with a narrow size distribution. Depending on the shape, the average particle size is of the order of some micrometers or some tens of micrometers. Similar powders of the lower carbides (Cr_2C, Cr_7C_3, and $Cr_{23}C_6$) can be prepared using still milder thermal treatments. A controlled morphology would be essential if these powders were to be used for preparing coatings by electrodeposition.

REFERENCES

1. L.E. Toth, *Transition Metal Carbides and Nitrides*, Academic Press, New York (1971).
2. G.G. Ferrier, A.R. Berzins, and N.M. Davey, *Platinum Metals Rev.* **29**, 175 (1985).
3. G.P. Demopoulos and G. Pouskouleli, *J. Metals* **40**, 46 (1988).

4. Y. Zenira, in *Precious Metals 1986*, ed. U.V. Rao, p. 409, IPMI, Allentown, PA (1986).
5. F. Fievet, J.P. Lagier, and M. Figlarz, *MRS Bull.* **24**, 29 (1989).
6. E. Matijevic, *Faraday Discuss.* **92**, 229 (1991).
7. S. Komarneni, R. Pidugu, Q.H. Li, and R. Roy, *J. Mater. Res.* **10**, 1687 (1995).
8. D. Thibaudon, M. Roubin, R.A. Paris, and J. Paris, *Planseeber. Pulvermetal.* **20**, 129 (1972).
9. A. Lerch and A. Rousset, *Thermochim. Acta* **232**, 233 (1994).
10. S. Loubière, Ch. Laurent, J.P. Bonino, and A. Rousset, *Mater. Res. Bull.* **30**, 1535 (1995).
11. S. Loubière, Ch. Laurent, J.P. Bonino, and A. Rousset, *J. Alloys Compd.* **243**, 59 (1996).
12. G. Leclercq, M. Kamal, J.-F. Lamonier, L. Feigenbaum, P. Malfoy, and L. Leclercq, *Appl. Catal., A: General* **121**, 169 (1995).